Thermoacoustic Transduction in Individual Suspended Carbon Nanotubes

Blake J. Mason,[†,∥] Shun-Wen Chang,[§] Jihan Chen,[†] Stephen B. Cronin,[†,‡,§] and Adam W. Bushmaker*[,∥]

Departments of [†]Electrical Engineering, [‡]Material Science, and [§]Physics and Astronomy, University of Southern California, Los Angeles, California 90089, United States and [∥]The Aerospace Corporation, El Segundo, California 90245, United States

ABSTRACT We report an experimental measurement of the acoustic signal emitted from an individual suspended carbon nanotube (CNT) approximate 2 μm in length, 1 nm in diameter, and 10^{-21} kg in mass. This system represents the smallest thermoacoustic system studied to date. By applying an AC voltage of 1.4 V at 8 kHz to the suspended CNT, we are able to detect the acoustic signal using a commercial microphone. The acoustic power detected is found to span a range from 0.1 to 2.4 attoWatts or 0.2 to 1 μPa of sound pressure. This corresponds to thermoacoustic efficiencies ranging from 0.007 to 0.6 Pa/W for the seven devices that were measured in this study. Here, the small lateral dimensions of these devices cause large heat losses due to thermal conduction, which result in the relatively small observed thermoacoustic efficiencies.

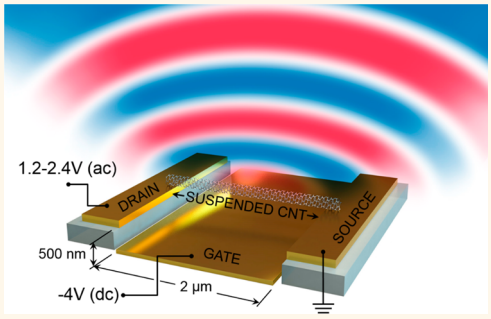

KEYWORDS: transduction · CNT · thermoacoustic · thermal conduction · loudspeaker

Most loudspeakers that are used today consist of an electromagnetic coil whose basic principle of operation dates back to 1924 invented by Rice and Kellogg.[1] These coils are bulky and cannot be integrated with standard silicon complementary metal oxide semiconductor (CMOS) fabrication techniques. The first CMOS-MEMS microspeaker was developed in 2002 by Gabriel and co-workers.[2] CMOS-MEMS micromachining techniques have enabled the integration of hundreds to thousands of microspeakers on a single chip together with sound optimization electronics. These CMOS-MEMS microspeakers typically have problems caused by nonlinearities, which can be controlled through membrane geometry design and tailoring of the material properties. More recently, an electrostatic graphene speaker consisting of multilayer graphene 7 mm in diameter was demonstrated by Zhou *et al.* and others.[3,4] The first fundamental work characterizing thermoacoustic transduction was performed by Arnold and Crandall at the Western Electric Company laboratories in 1917.[5] Their work focused on sound production *via* thermoacoustic transduction from a 700 nm thick Pt film, which they called the "Thermophone". They found that when an AC current is passed through a thin conductor, periodic heating at the surface causes periodic thermal expansion in the surrounding medium, which creates acoustic waves that propagate away from the surface. Acoustic emission was also reported in single 5 cm^2 filaments made of carbon/polycarbonate.[6] More recently, Xiao *et al.*[7] and others[8−11] have demonstrated intense thermoacoustic energy conversion using carbon nanotube (CNT) films. Thermoacoustic transduction has also been demonstrated in other thin-film structures, such as mesh-films of silver nanowires[12] and graphene,[13−15] and there are several recent patents in this area[16−18] indicating commercial interest in the application of this technology.

While several micro- and nanoscale systems have been studied, as described above, the minimum length scale of an object that can emit sound audible with standard macroscopic sensors has not been established. Individual carbon nanotubes (CNTs) represent one of the smallest possible conductors with electrical, mechanical, and thermal properties that exceed most known bulk materials. Two particularly unique physical properties of

* Address correspondence to abushmaker@gmail.com.

Received for review February 18, 2015 and accepted May 11, 2015.

Published online May 11, 2015
10.1021/acsnano.5b01119

CNTs are their extremely low heat capacity compared to that of other conductors and their high surface to volume ratio.[19] The combination of these two properties makes single-walled CNTs especially effective for thermoacoustic transduction.

Here, we report the first observation of thermoacoustic transduction from an individual molecule (1 nm in diameter), which is 4 orders of magnitude smaller than any previous thermoacoustic system studied, reducing the CNT-based thermoacoustic loudspeaker to its smallest fundamental element, a single CNT. This work tests assumptions made in previous models used to describe 2D thermoacoustic films. We correlate the thermoacoustic efficiencies of these nanotube devices with their electrical impedance in order to understand loss mechanisms.

RESULTS

Figure 3a shows the AC voltage detected in the microphone (at 16 kHz) plotted as a function of time. A clear increase from a baseline of 2 nV to 25 nV is seen after the AC input signal (1.4 V_{rms}) is applied to the CNT. The sensitivity of our microphone is 32 mV/Pa. From this value, we can convert the detected voltage of 23 nV (after subtracting the 2nV baseline) to a sound pressure level of −28 dB. The acoustic power P is represented as

$$P = \frac{Ap^2}{Z} \quad (1)$$

where A is the total area the sound waves spread out to at the distance measured, p is the sound pressure detected, and Z is the acoustic impedance of nitrogen gas (Z = 406 N·s/m^3 at 300 K). From here, we can calculate the acoustic power corresponding to the 23 nV detected in the microphone to a sound power of 1.3 aW (1.3 × 10^{-18} W). The same measurement was repeated on seven different devices. Figure 3b shows the output acoustic pressure plotted as a function of the input power for four different devices. They all exhibit linear relationships between the input power and output pressure, as expected.

To fit the experimental data obtained from their Pt thin films, Arnold and Crandall derived the first model for thermoacoustic transduction relating the RMS sound pressure generated (p_{rms}) to the input electrical power (p_{input}):

$$p_{rms} = \frac{\sqrt{\alpha}\rho_0}{2\sqrt{\pi}T_0} \cdot \frac{1}{r} \cdot P_{input} \cdot \frac{\sqrt{f}}{C_s} \quad (2)$$

where C_s is the heat capacity per unit area of the CNT, r is the distance between the conductor and the microphone, and f is the frequency of the AC driving voltage. T_0, α, and ρ are the ambient temperature, thermal diffusivity of the surrounding gas, and density, respectively. This equation defines an inverse relationship between the heat capacity per unit area C_s of a material

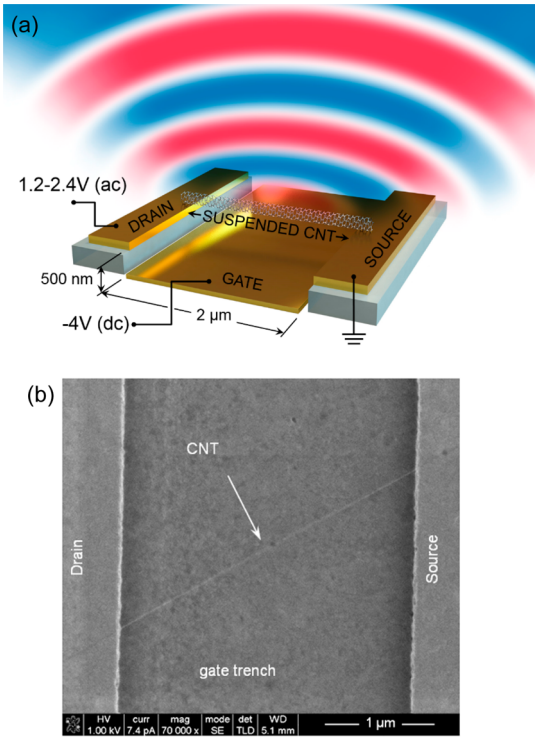

Figure 1. (a) Schematic diagram of our device geometry, which contains a source, a drain, and a gate electrode. (b) SEM image showing one of our individual suspended carbon nanotube devices.

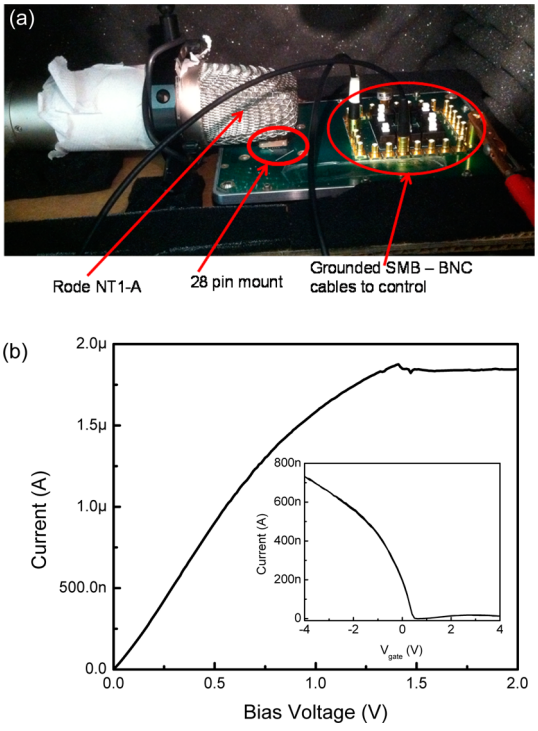

Figure 2. (a) Picture of the experimental setup inside the hemianechoic chamber. (b) Current−bias voltage characteristics, and the inset shows current−gate voltage characteristics, of one of our individual suspended CNT FET devices.

and its potential as a thermoacoustic transducer. Single-walled carbon nanotubes with an ultralow C_s

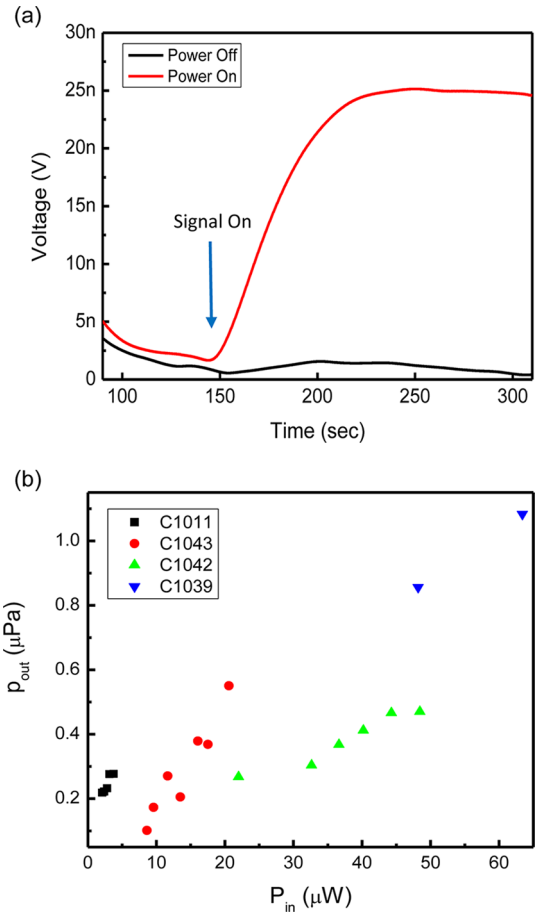

Figure 3. (a) Voltage detected by the microphone when an input AC voltage is applied to the CNT device. The black line represents the baseline signal when there is no input voltage applied. (b) The measured acoustic pressure plotted as a function of the electrical input power for several different devices, which all show a linear relation between input power and output pressure.

(typically 10^{-4} J/K·m^2) are therefore an ideal material for this transduction as opposed to platinum foil, which has a substantially higher C_s (typically 2 J/K·m^2). The input electrical power P_{input} is calculated as $I_{sd} \cdot V_{sd}$. At high source–drain bias voltages, the majority of the power dissipation occurs in the CNT due to optical phonon scattering, allowing us to neglect power dissipated in the contacts.

More recently, Xiao *et al.* modified the Arnold and Crandall model to fit their thermoacoustic data taken from carbon nanotube thin films. This revised model[7] takes into account the rate of heat loss per unit area of the conductor per unit rise of temperature relative to the surrounding environment, β_o, as given by the following equation:

$$p_{rms} = \frac{\sqrt{\alpha}\rho_0}{2\sqrt{\pi}T_0} \cdot \frac{1}{r} \cdot P_{input} \cdot \frac{\sqrt{f}}{C_S} \cdot \frac{\frac{f}{f_2}}{\sqrt{\left(1+\sqrt{\frac{f}{f_1}}\right)^2 + \left(\frac{f}{f_2}+\sqrt{\frac{f}{f_1}}\right)^2}} \quad (3)$$

$$f_1 = \frac{\alpha\beta_0^2}{\pi\kappa^2} \quad (4)$$

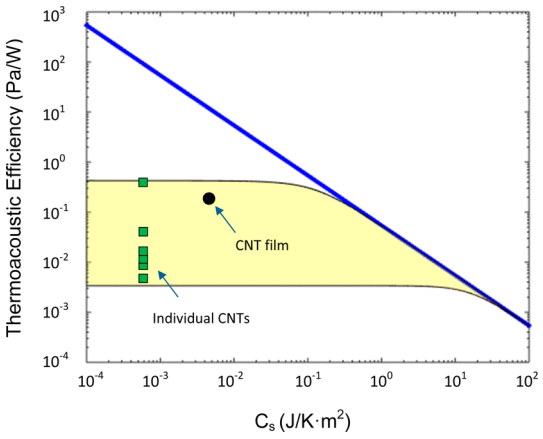

Figure 4. Dependence of the thermoacoustic efficiency (p_{rms}/P_{in}) on the heat capacity per unit area (C_s) calculated according to Arnold and Crandall's model (blue line) and Xiao's model (yellow shaded region). The black dot indicates the value from CNT films, and the green squares correspond to the experimental values observed from our individual suspended CNT devices.

$$f_2 = \frac{\beta_0}{\pi C_s} \quad (5)$$

where κ is the thermal conductivity of the surrounding gas environment.

We define the thermoacoustic efficiency as the ratio of the sound pressure generated to the input electrical power (p_{rms}/P_{in}). In Figure 4, we show the theoretical prediction of both the Arnold–Crandall model and the Xiao model. The black dot indicates the experimental value for a CNT film from Xiao's paper. The green squares indicate the experimental values obtained from our single CNT thermoacoustic devices, which span a wide range from 0.007 to 0.56 Pa/W. This is 3–4 orders of magnitude below the Arnold and Crandall model. One of the main reasons for this discrepancy is the high temperatures (>1000 K) reached in these individual CNT devices, which causes a large portion of the heat generated in the CNT to be conducted to the supporting substrate, thus decreasing the thermoacoustic efficiency of the system. In this model, all of the heat losses are lumped together into one term, β_o, including both convection and conduction. Therefore, within this simple model, we are unable to isolate the one-dimensional heat transport along the nanotube. However, on the basis of our previous work, we have separated these two effects using spatially resolved Raman spectroscopy, and found that 50%–60% of the heat dissipated in these suspended nanotubes is removed by its surrounding gas molecules,[20] while the remaining 40–50% is lost through thermal conduction. Radiative loses were found to be negligible. These conductive heat loss mechanisms are not as significant a problem in large, disordered network films of CNTs, since the thermal conductivity to the substrate is considerably lower than in the case of our individual CNT devices. Therefore, we expect that the thermoacoustic

efficiency can be improved by increasing the thermal resistance of the system, for example, by using longer suspended nanotubes or increasing the thermal contact resistance. Another related problem arises when C_s is small. Here, there is inherently more heat loss to conduction to the underlying substrate due to the short aspect ratio of our devices. By adjusting the heat exchange due to thermal conduction β_o (and hence f_1 and f_2) to span a range from 5000 to 800000 W/m^2·K, the Xiao model can be used to fit an upper and lower bound of our experimental data, as plotted in the yellow shaded region in Figure 4. These values are 2−4 orders of magnitude larger than those of Xiao *et al.* (β_o = 29 W/m^2·K for 1-layer CNT film), who used the bulk value of the thermal conductivity of the CNT film ~200 W/m·K.[21] However, the heat dissipation/conduction in our devices is dominated by the extremely high thermal conductivity of these individual suspended CNT, which is around 3600 W/m·K.[22]

Figure 5 shows a graph of the sound pressure generated from several different types of acoustic transducers plotted as a function of device volume. The conventional electromagnetic coil has the largest volume on the order of 500 cm^3 and a typical sensitivity rating of about 90 dB, corresponding to an RMS sound pressure of 0.6 Pa. For a CMOS-MEMS speaker, the membrane volume is around 0.06 mm^3, which produces a sound pressure of 0.1 Pa with a 75 V electrical pulse.[2] This corresponds to an electrical input power of about 8 mW and a conversion efficiency of 12.5 Pa/W. For a monolayer graphene thermoacoustic device,[15] the graphene volume is 1.75 × 10^{-13} m^3 and the sound pressure produced is 50 mPa with 0.02 W input power. This corresponds to a conversion efficiency of 2.5 Pa/W. Our individual CNT devices have a volume of 6 × 10^{-24} m^3 and represent the smallest thermoacoustic devices studied to date. Under 63 μW of electrical excitation, they produce a sound pressure of 0.8 μPa, which corresponds to a thermoacoustic efficiency of 0.01 Pa/W.

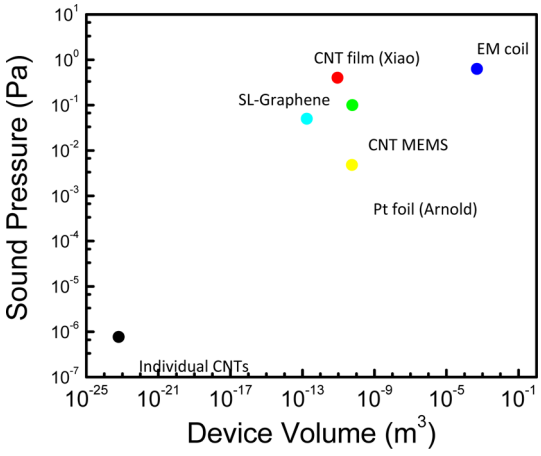

Figure 5. Sound pressure plotted as a function of device volume for various acoustic transducers.

CONCLUSION

We have reported the smallest acoustic system to date, consisting of a 2 μm long individual single walled carbon nanotube. Seven devices were measured, which exhibited electrical-to-acoustic conversion efficiencies ranging from 0.007 to 0.56 Pa/W. The observed thermoacoustic transduction efficiencies are relatively small, mainly due to the small lateral dimensions and high thermal conductivity of these carbon nanotubes, which result in substantial losses due to thermal conduction to the supporting substrate. By adjusting the thermal conductance parameter in previous models of thermoacoustic transduction, upper and lower bounds can be fit to our experimental data, further substantiating the role of thermal heat losses in the low thermoacoustic efficiencies observed in these individual carbon nanotube devices.

METHODS

Suspended CNTs are grown by chemical vapor deposition (CVD) on prepatterned wafers using ferric nitrate catalyst at 825 °C as reported previously.[23−25] Before growth, platinum source and drain electrodes are patterned on a $Si/SiO_2/Si_3N_4$ wafer, together with a gate electrode in a 800 nm deep, 2−5 μm wide trench etched into the wafer.[26] The resulting field effect transistor (FET) device geometry is illustrated in Figure 1a. The nanotube growth is the final step in this sample fabrication process, which ensures that these nanotubes are not contaminated by any chemical residues from the lithographic fabrication processes. Figure 1b shows a scanning electron microscope (SEM) image of one of our CNT devices. The devices are then probed and wire-bonded to a 14-pin chip mount. Mounted chips are placed inside a home-built hemianechoic chamber, as shown in Figure 2a. A nitrogen gas environment is used to purge the anechoic chamber (1 atm) to avoid oxidation of the CNT by oxygen in air. An ultralow noise RØDE NT1-A cardioid microphone was placed 12 mm directly above the chip. The output of the microphone was directly connected to a Stanford Research SR830 DSP lock-in amplifier *via* BNC cable. First, the lock-in time constant was set to 300 ms to allow for quick decay of the residual noise in the microphone. Next, the time constant was increased to 10 s and an AC bias voltage between 1.2 V_{rms} and 2.4 V_{rms} was applied across the source and drain electrodes of the CNT device at a driving frequency of 8 kHz. The 8 kHz driving frequency was chosen to optimize the sensitivity of the microphone, which peaks around 16 kHz. On the basis of our previous work using Raman spectroscopy, we expect these suspended CNTs to reach temperatures of over 1000 K under these large applied bias voltages.[20,25,27,28] Figure S1 in the Supporting Information shows some relevant Raman spectra taken on an individual suspended carbon nanotube under various applied bias potentials.[28] The second harmonic of the driving frequency was set as the reference frequency for the input signal to the lock-in amplifier (*i.e.*, 16 kHz), since the frequency doubles because the CNT heats up twice per cycle during thermoacoustic transduction ($P = I^2R$). Negative DC gate voltages (V_g = −4 V) were applied in order to minimize the contact and CNT resistance. Figure 2b shows the typical electron transport characteristics of our CNT devices. The saturation of the current at high bias indicates heating in the device, as studied previously.[29−31] The inset shows the current−gate voltage characteristics with a charge neutrality point at 0.5 V.

A total of seven devices, including both semiconducting and quasi-metallic nanotubes were found to have measurable thermoacoustic signals.

Conflict of Interest: The authors declare no competing financial interest.

Acknowledgment. This research was supported by DOE Award No. DE-FG02-07ER46376. The portion of the work conducted at The Aerospace Corporation was funded by the Independent Research and Development Program at The Aerospace Corporation.

Supporting Information Available: Raman shift data and corresponding temperature from a single carbon nanotubes under various applied bias voltages. The Supporting Information is available free of charge on the ACS Publications website at DOI: 10.1021/acsnano.5b01119.

REFERENCES AND NOTES

1. Rice, C. W.; Kellogg, E. W. Notes on the Development of a New Type of Hornless Loud Speaker. *Trans. Am. Inst. Electr. Eng.* **1925**, *44*, 461–480.
2. Diamond, B. M.; Neumann Jr, J. J.; Gabriel, K. J. Digital Sound Reconstruction Using Arrays of CMOS-MEMS Microspeakers, *IEEE Int. Conf. Micro Electro Mech. Syst.*, 15*th*: **2002**; pp 292−295.
3. Zhou, Q.; Zettl, A. Electrostatic Graphene Loudspeaker. *Appl. Phys. Lett.* **2013**, *102*, 223109.
4. Xu, S.; Man, B.; Jiang, S.; Chen, C.; Yang, C.; Liu, M.; Gao, X.; Sun, Z.; Zhang, C. Flexible and Transparent Graphene-Based Loudspeakers. *Appl. Phys. Lett.* **2013**, *102*, 151902.
5. Arnold, H. D.; Crandall, I. B. The Thermophone as a Precision Source of Sound. *Phys. Rev.* **1917**, *10*, 22–38.
6. Ma, B.; Schadler, L.; Laird, C.; Figueroa, J. Acoustic Emission in Single Filament Carbon/Polycarbonate and Kevlar/Olycarbonate Composites under Tensile Deformation. *Polym. Compos.* **1990**, *11*, 211–216.
7. Xiao, L.; Chen, Z.; Feng, C.; Liu, L.; Bai, Z. Q.; Wang, Y.; Qian, L.; Zhang, Y. Y.; Li, Q. Q.; Jiang, K. L.; *et al.* Flexible, Stretchable, Transparent Carbon Nanotube Thin Film Loudspeakers. *Nano Lett.* **2008**, *8*, 4539–4545.
8. Barnard, A. R.; Jenkins, D. M.; Brungart, T. A.; McDevitt, T. M.; Kline, B. L. Feasibility of a High-Powered Carbon Nanotube Thin-Film Loudspeaker. *J. Acoust. Soc.Am.* **2013**, *134*, EL276–EL281.
9. Suzuki, K.; Sakakibara, S.; Okada, M.; Neo, Y.; Mimura, H.; Inoue, Y.; Murata, T., Study of Carbon-Nanotube Web Thermoacoustic Loud Speakers. *Jpn. J. Appl. Phys.* **2011**, *50*.
10. Aliev, A. E.; Lima, M. D.; Fang, S.; Baughman, R. H. Underwater Sound Generation Using Carbon Nanotube Projectors. *Nano Lett.* **2010**, *10*, 2374–2380.
11. Nasibulin, A. G.; Kaskela, A.; Mustonen, K.; Anisimov, A. S.; Ruiz, V.; Kivisto, S.; Rackauskas, S.; Timmermans, M. Y.; Pudas, M.; Aitchison, B. Multifunctional Free-Standing Single-Walled Carbon Nanotube Films. *ACS Nano* **2011**, *5*, 3214–3221.
12. Tian, H.; Xie, D.; Yang, Y.; Ren, T.-L.; Lin, Y.-X.; Chen, Y.; Wang, Y.-F.; Zhou, C.-J.; Peng, P.-G.; Wang, L.-G. Flexible, Ultrathin, and Transparent Sound-Emitting Devices Using Silver Nanowires Film. *Appl. Phys. Lett.* **2011**, *99*, 253507.
13. Suk, J. W.; Kirk, K.; Hao, Y.; Hall, N. A.; Ruoff, R. S. Thermoacoustic Sound Generation from Monolayer Graphene for Transparent and Flexible Sound Sources. *Adv. Mater.* **2012**, *24*, 6342–6347.
14. Tian, H.; Ren, T.-L.; Xie, D.; Wang, Y.-F.; Zhou, C.-J.; Feng, T.-T.; Fu, D.; Yang, Y.; Peng, P.-G.; Wang, L.-G. Graphene-on-Paper Sound Source Devices. *ACS Nano* **2011**, *5*, 4878–4885.
15. Tian, H.; Xie, D.; Yang, Y.; Ren, T.-L.; Wang, Y.-F.; Zhou, C.-J.; Peng, P.-G.; Wang, L.-G.; Liu, L.-T. Single-Layer Graphene Sound-Emitting Devices: Experiments and Modeling. *Nanoscale* **2012**, *4*, 2272–2277.
16. Jiang, K.-L.; Lin, X.-Y.; Xiao, L.; Fan, S.-S. Thermoacoustic Device. US Patent 8842857 B2, **2014**.
17. Wang, Y.-Q.; Qian, L.; Feng, C.; Liu, L. Thermoacoustic Device. US Patent 20110274297 A1, **2013**.
18. Wei, Y.; Fan, S.-S. Thermoacoustic Device. US Patent 20140140547 A1, **2013**.
19. Li, J.; Lu, Y. J.; Ye, Q.; Cinke, M.; Han, J.; Meyyappan, M. Carbon Nanotube Sensors for Gas and Organic Vapor Detection. *Nano Lett.* **2003**, *3*, 929–933.
20. Hsu, I. K.; Pettes, M. T.; Aykol, M.; Shi, L.; Cronin, S. B. The Effect of Gas Environment on Electrical Heating in Suspended Carbon Nanotubes. *J. Appl. Phys.* **2010**, *108*, 084307.
21. Hone, J.; Llaguno, M.; Nemes, N.; Johnson, A.; Fischer, J.; Walters, D.; Casavant, M.; Schmidt, J.; Smalley, R. Electrical and Thermal Transport Properties of Magnetically Aligned Single Wall Carbon Nanotube Films. *Appl. Phys. Lett.* **2000**, *77*, 666–668.
22. Hone, J.; Whitney, M.; Piskoti, C.; Zettl, A. Thermal Conductivity of Single-Walled Carbon Nanotubes. *Phys. Rev. B* **1999**, *59*, R2514.
23. Chang, S.-W.; Dhall, R.; Amer, M.; Sato, K.; Saito, R.; Cronin, S. Evidence for Structural Phase Transitions and Large Effective Band Gaps in Quasi-metallic Ultra-Clean Suspended Carbon Nanotubes. *Nano Res.* **2013**, *6*, 736–744.
24. Dhall, R.; Chang, S.-W.; Liu, Z.; Cronin, S. B. Pronounced Electron-Phonon Interactions in Ultraclean Suspended Carbon Nanotubes. *Phys. Rev. B* **2012**, *86*, 045427.
25. Bushmaker, A. W.; Deshpande, V. V.; Hsieh, S.; Bockrath, M. W.; Cronin, S. B. Direct Observation of Born−Oppenheimer Approximation Breakdown in Carbon Nanotubes. *Nano Lett.* **2009**, *9*, 607–611.
26. Bushmaker, A. W.; Deshpande, V. V.; Hsieh, S.; Bockrath, M. W.; Cronin, S. B. Large Modulations in the Intensity of Raman-Scattered Light from Pristine Carbon Nanotubes. *Phys. Rev. Lett.* **2009**, *103*, 67401.
27. Deshpande, V. V.; Hsieh, S.; Bushmaker, A. W.; Bockrath, M.; Cronin, S. B. Spatially Resolved Temperature Measurements of Electrically Heated Carbon Nanotubes. *Phys. Rev. Lett.* **2009**, *102*, 105501.
28. Liu, Z.; Bushmaker, A.; Aykol, M.; Cronin, S. B. Thermal Emission Spectra from Individual Suspended Carbon Nanotubes. *ACS Nano* **2011**, *5*, 4634–4640.
29. Pop, E.; Mann, D.; Cao, J.; Wang, Q.; Goodson, K.; Dai, H. Negative Differential Conductance and Hot Phonons in Suspended Nanotube Molecular Wires. *Phys. Rev. Lett.* **2005**, *95*, 155505.
30. Bushmaker, A. W.; Deshpande, V. V.; Bockrath, M. W.; Cronin, S. B. Direct Observation of Mode Selective Electron−Phonon Coupling in Suspended Carbon Nanotubes. *Nano Lett.* **2007**, *7*, 3618–3622.
31. Amer, M.; Bushmaker, A.; Cronin, S. Anomalous Kink Behavior in the Current−Voltage Characteristics of Suspended Carbon Nanotubes. *Nano Res.* **2012**, *5*, 172–180.